High-energy signatures of nuclear processes in supernovae

NAVI meeting, 17.12.2013, GSI Darmstadt

Alexander Summa

Outline

High energy observables of nuclear processes in supernovae

⇕

Diagnostic tools for conclusions on astrophysical models

Two examples:

1. Nuclear lines as a fingerprint of hadronic cosmic rays
2. High-energy observables of Type Ia supernovae
   - Gamma-ray emission
   - X-ray line emission

Outline

High energy observables of nuclear processes in supernovae

⇕

Diagnostic tools for conclusions on astrophysical models

Two examples:

1. Nuclear lines as a fingerprint of hadronic cosmic rays
2. High-energy observables of Type Ia supernovae
   – Gamma-ray emission
   – X-ray line emission

The spectrum of cosmic rays

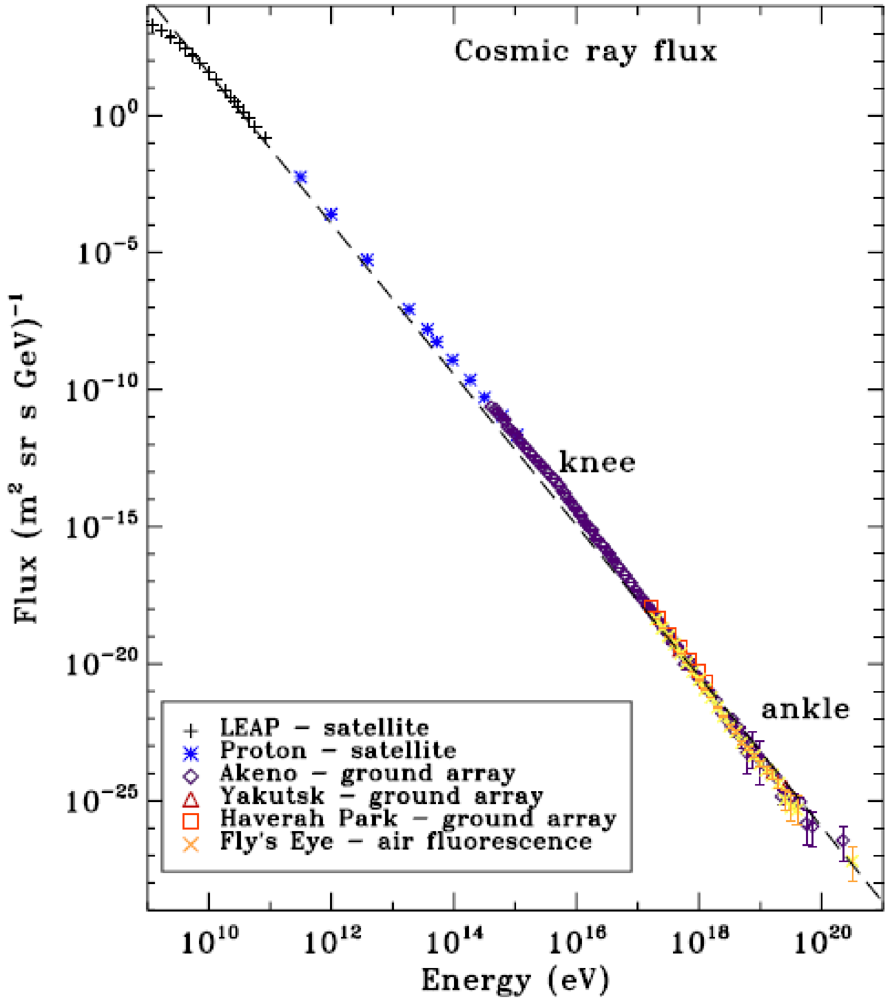

Particle fluxes of cosmic rays as observed by different instruments in dependence on the particle energy **(Helder et al. 2012)**

General picture:

- Cosmic rays with energies below the "knee" originate within the Galaxy

→ Possible source: Diffusive particle acceleration processes at supernova remnant shocks

- Cosmic rays with energies above the "knee" have an extragalactic origin

The supernova remnant Cassiopeia A

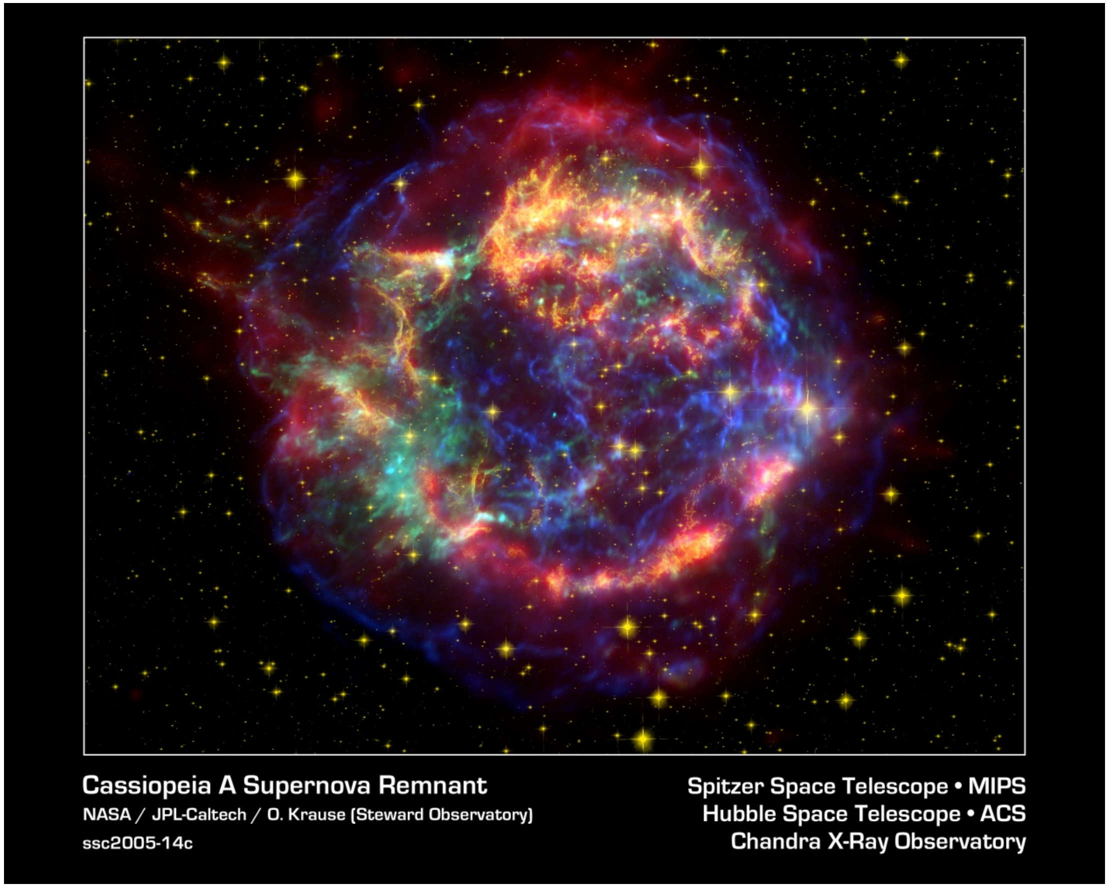

False-colour picture of the supernova remnant Cas A:

- Spitzer Space Telescope (red): warm dust in the outer shell (several 100 K)
- Hubble Space Telescope (yellow): filamentary structures of hot gases (about 10^4 K)
- Chandra X-ray Observatory (green and blue): hot gases up to 10^6 K

→ Emission at most wave-lengths is dominated by „Bright Ring“ which is formed when ejecta encounter Cas A‘s reverse shock and are heated and ionized.

Leptonic vs. hadronic emission models

Most promising model for the origin of galactic cosmic rays: Diffusive shock acceleration operating at expanding supernova remnant shells.

→ Gamma rays as a signature for hadronic interactions

→ But: Disentanglement of hadronic and leptonic contributions to the observed gamma-ray emission is difficult.

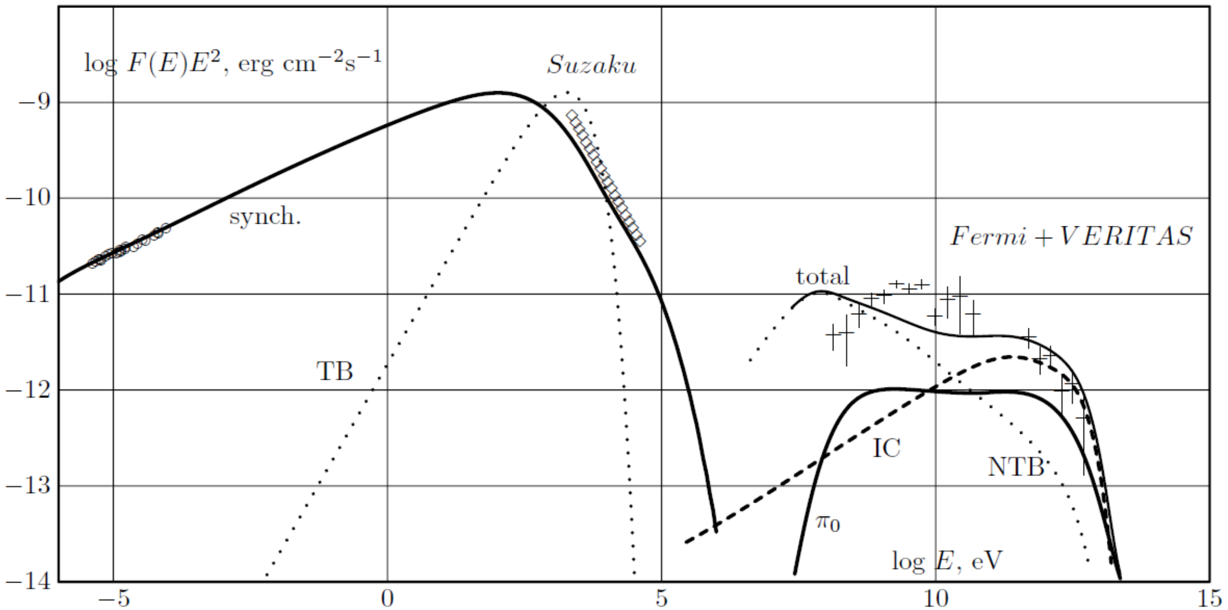

Modeling of the SED of Cas A with a leptonic emisson model:

Shown in the GeV–TeV bands are the contributions of non-thermal-bremsstrahlung and inverse-Compton scattering processes.

Zirakashvili et al. (2013)

Julius-Maximilians-UNIVERSITÄT WÜRZBURG

Leptonic vs. hadronic emission models

Most promising model for the origin of galactic cosmic rays: Diffusive shock acceleration operating at expanding supernova remnant shells.

→ Gamma rays as a signature for hadronic interactions

→ But: Disentanglement of hadronic and leptonic contributions to the observed gamma-ray emission is difficult.

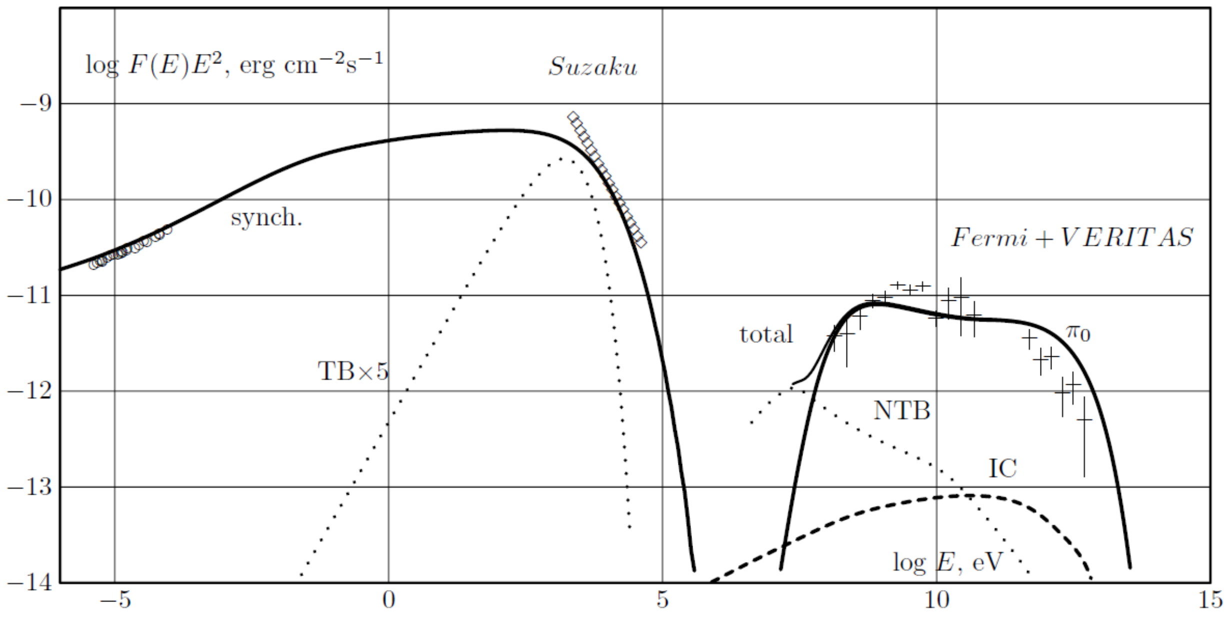

Modeling of the SED of Cas A with a hadronic emisson model:

Shown in the GeV–TeV bands are the contributions of non-thermal bremsstrahlung and inverse-Compton scattering processes as well as pion decays.

Zirakashvili et al. (2013)

Nuclear de-excitation lines

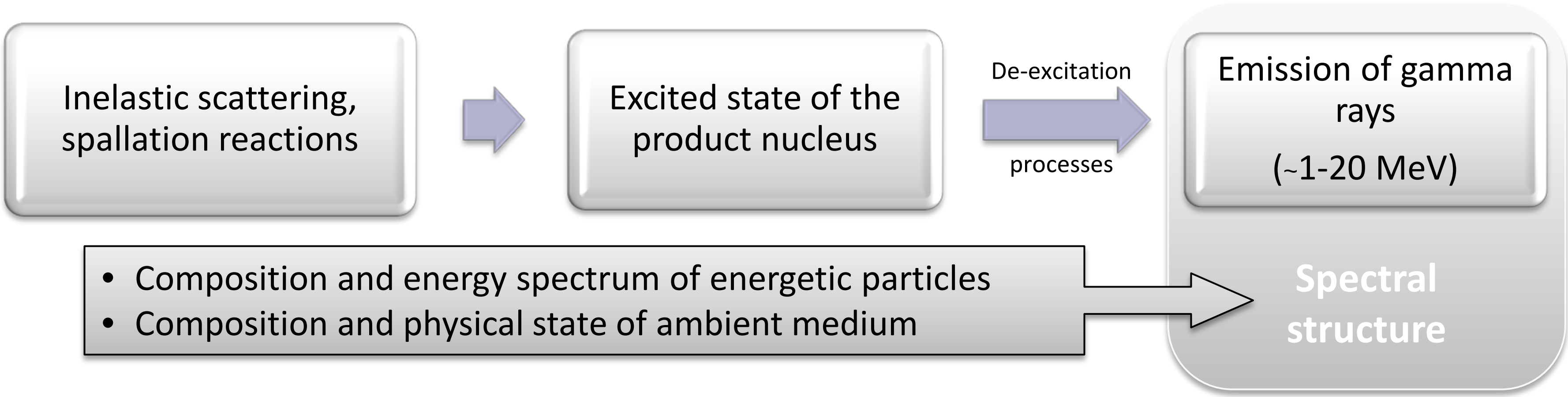

Nuclear gamma-ray lines:

→ indicate presence of cosmic rays in interstellar space or in localized objects

→ are best suited to the study of low energy cosmic rays (E<100 MeV)

Determination of gamma-ray line profiles:

→ probability of photon emission can be written as:

$$\mathrm{d}P_\gamma = n_i v \frac{\mathrm{d}\sigma}{\mathrm{d}\Omega^*}(E, \theta_r^*)\,\mathrm{d}(\cos\theta_r^*)\,\mathrm{d}\phi_r\; g(E, \theta_r^*, \theta_0, \phi_r - \phi_0)\,\mathrm{d}(\cos\theta_0)\,\mathrm{d}\phi_0$$

Nuclear de-excitation line spectrum of Cassiopeia A

Target abundances from X-ray and optical spectroscopy:

ratio	mean	rms
H/Si	$< 2.29 \times 10^{-5}$	-
He/Si	$< 4.93 \times 10^{-3}$	-
C/Si	1.76	0.88
O/Si	1.69	1.37
Ne/Si	0.24	0.37
Mg/Si	0.16	0.15
S/Si	1.25	0.24
Ar/Si	1.38	0.48
Ca/Si	1.46	0.68
FeL/Si	0.19	0.65
FeK/Si	0.60	0.51
Ni/Si	1.67	5.52

Mean measured abundance mass ratios and rms scatter resp. upper limits according to the results of **Willingale et al. (2002)**, **Docenko & Sunyaev (2010)** and **Chevalier & Kirshner (1979)**.

→ Heavy-element enriched Wolf-Rayet wind mixed with supernova ejecta

Spectrum of accelerated particles from nonlinear kinetic acceleration models:

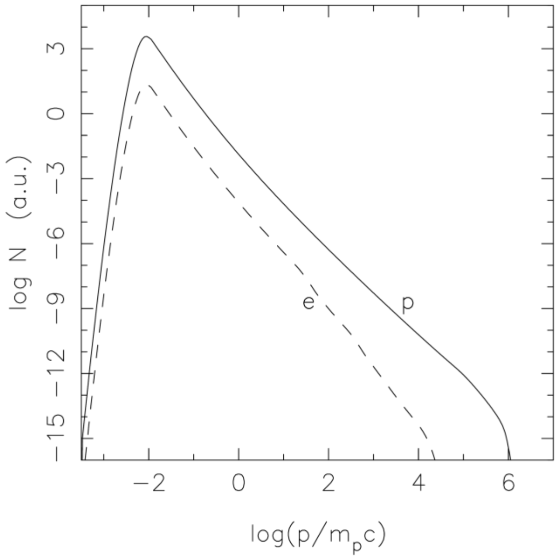

Overall CR proton (*solid line*) and electron (*dashed line*) spectra as function of momentum according to the results of **Berezhko et. al (2003)** for Cas A.

→ Consistent with gamma-ray measurements

Nuclear de-excitation line spectrum of Cassiopeia A

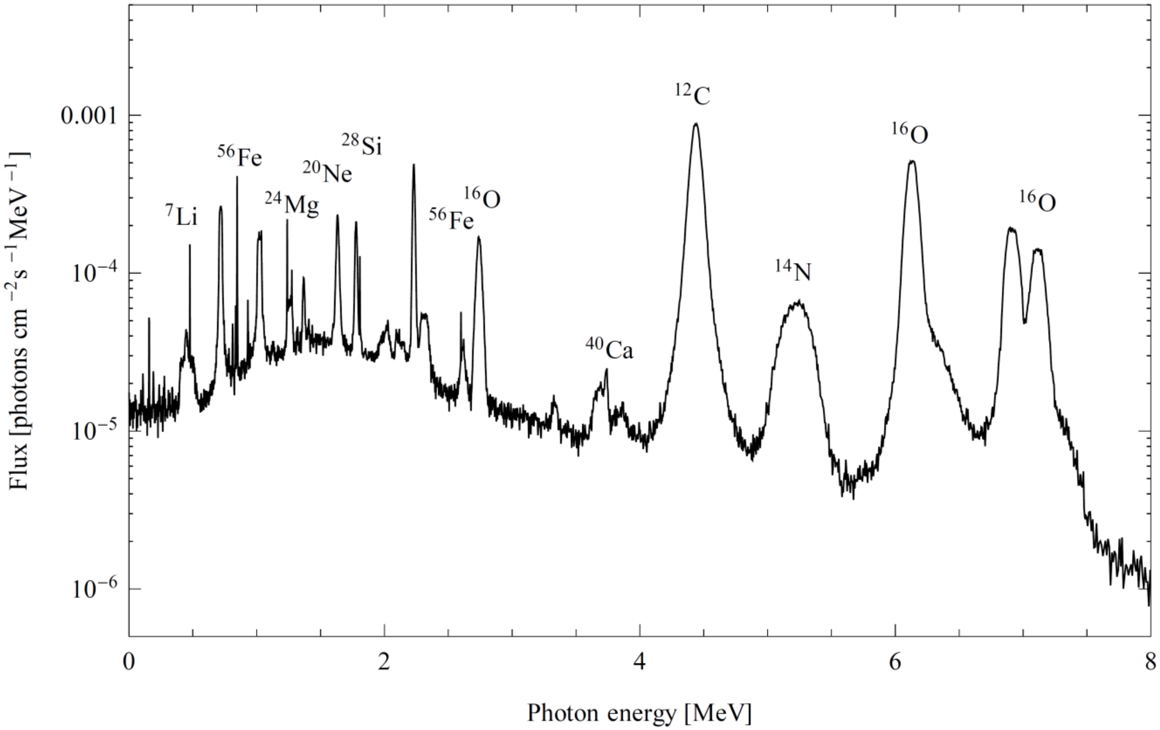

Calculated gamma-ray spectrum **Summa et al. (2011)** for the specific case of Cas A using the Monte-Carlo code by **Kozlovsky, Murphy & Ramaty (2002)**.

- Unresolved gamma-rays from heavy nuclei and lines from long-term radioactive nuclei are also included.
- Consideration of recoiling target particles.

→ Significant broadening of the lines.

- Detailed line characteristics are always dependent on the precise knowledge of the supernova ejecta‘s composition.

→ Flux of nuclear de-excitation lines would be clearly detectable by a future gamma-ray mission with enhanced sensitivity in the MeV range.

Detection prospects

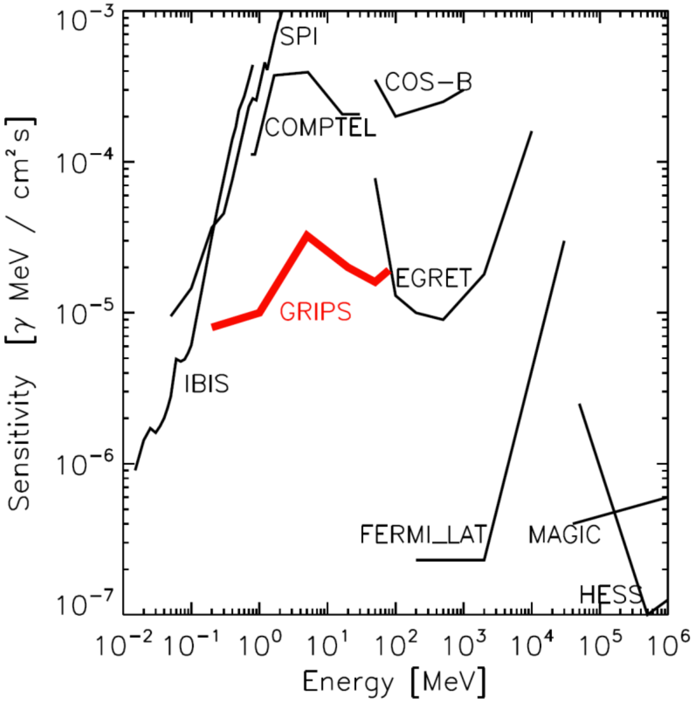

Current sensitivities (black) for instruments in the high energy range revealing a gap in the MeV range. The estimated sensitivity for the proposed GRIPS mission (red) is also shown **(Greiner et al. 2012)**.

- Unresolved gamma-rays from heavy nuclei and lines from long-term radioactive nuclei are also included.
- Consideration of recoiling target particles.

→ Significant broadening of the lines.

- Detailed line characteristics are always dependent on the precise knowledge of the supernova ejecta's composition.

→ Flux of nuclear de-excitation lines would be clearly detectable by a future gamma-ray mission with enhanced sensitivity in the MeV range.

Outline

High energy observables of nuclear processes

⇕

Diagnostic tools for conclusions on astrophysical models

Two examples:

1. Nuclear lines as a fingerprint of hadronic cosmic rays
2. High-energy observables of Type Ia supernovae
   - Gamma-ray emission
   - X-ray lines

Astrophysical significance of Type Ia supernovae

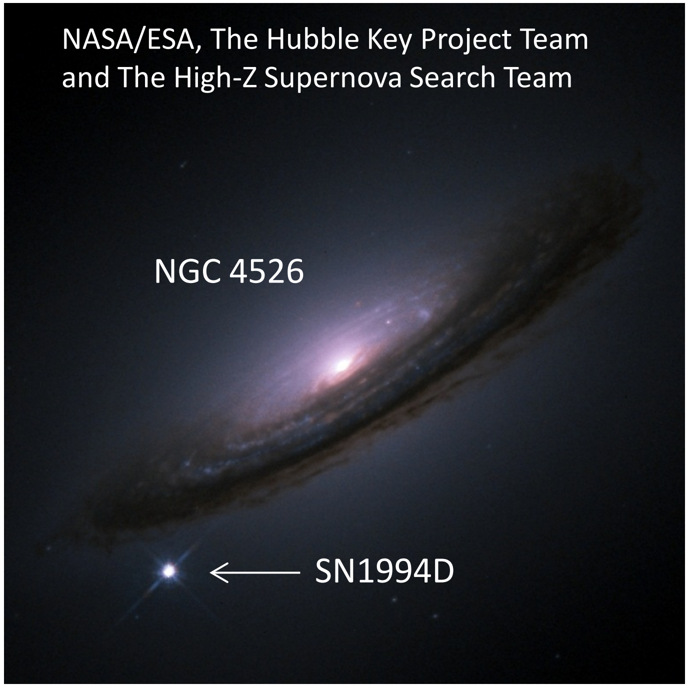

Type Ia supernovae are relevant for

- observational cosmology
- the cosmic cycle of matter
- triggering star formation
- understanding binary stellar evolution
- ...

General agreement: Type Ia supernovae are the result of thermonuclear explosions of carbon-oxygen white dwarfs

But: Many questions concerning the progenitor and explosion scenarios remain open

Progenitor models of Type Ia supernovae

Single degenerate scenario

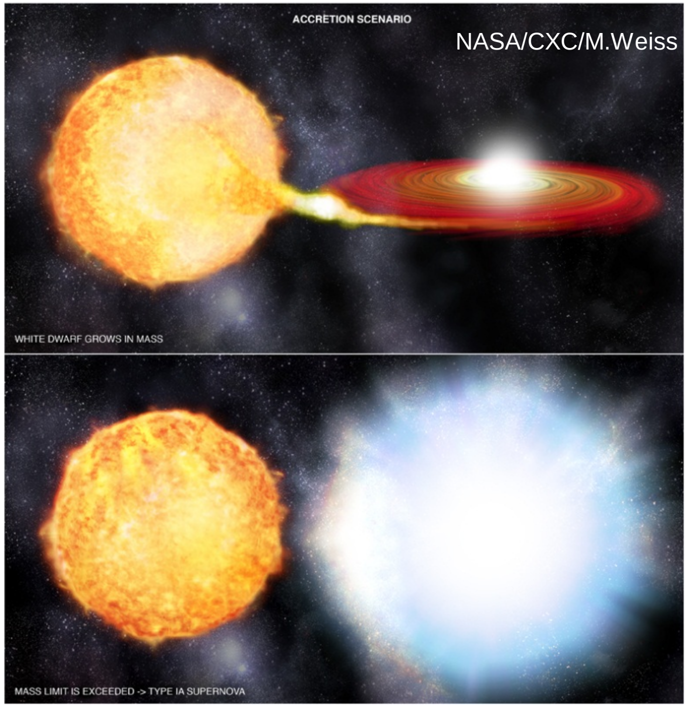

- White dwarf accretes mass from a companion star through Roche-lobe overflow or strong stellar winds
- $M_{\mathrm{WD,final}} \approx 1.4\, M_{\odot}$

Progenitor models of Type Ia supernovae

Single degenerate scenario

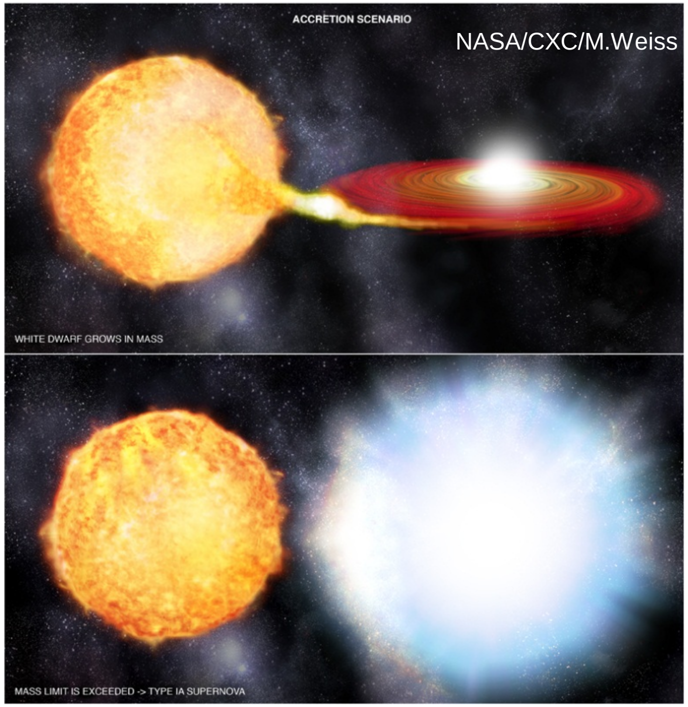

- White dwarf accretes mass from a companion star through Roche-lobe overflow or strong stellar winds
- $M_{\mathrm{WD,final}} \approx 1.4\,M_\odot$

Double degenerate scenario

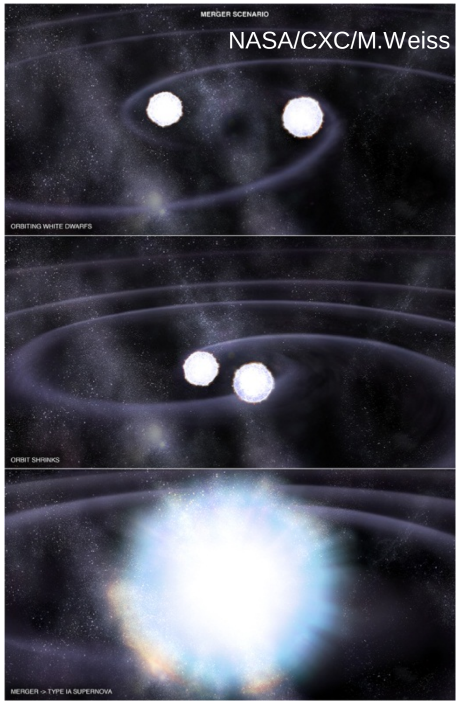

- Two white dwarfs merge, lighter white dwarf is accreted onto more massive one
- $M_{\mathrm{tot}} > 1.4\,M_\odot$

3D simulations of Type Ia supernovae

Modeling pipeline:

Progenitor scenario → Hydrodynamical simulation → Nucleosynthesis calculation → Radiative transfer calculations → Observables (lightcurves, spectra)

3D simulations of Type Ia supernovae

Modeling pipeline:

Progenitor scenario → Hydrodynamical simulation → Nucleosynthesis calculation → Radiative transfer calculations → Observables (lightcurves, spectra)

First simulation
(single degenerate scenario)

Delayed detonation model:
(Seitenzahl et al. 2012)

- Total ejecta mass: $1.4\,M_{\odot}$
- Produced amount of ^{56}Ni: $0.6\,M_{\odot}$

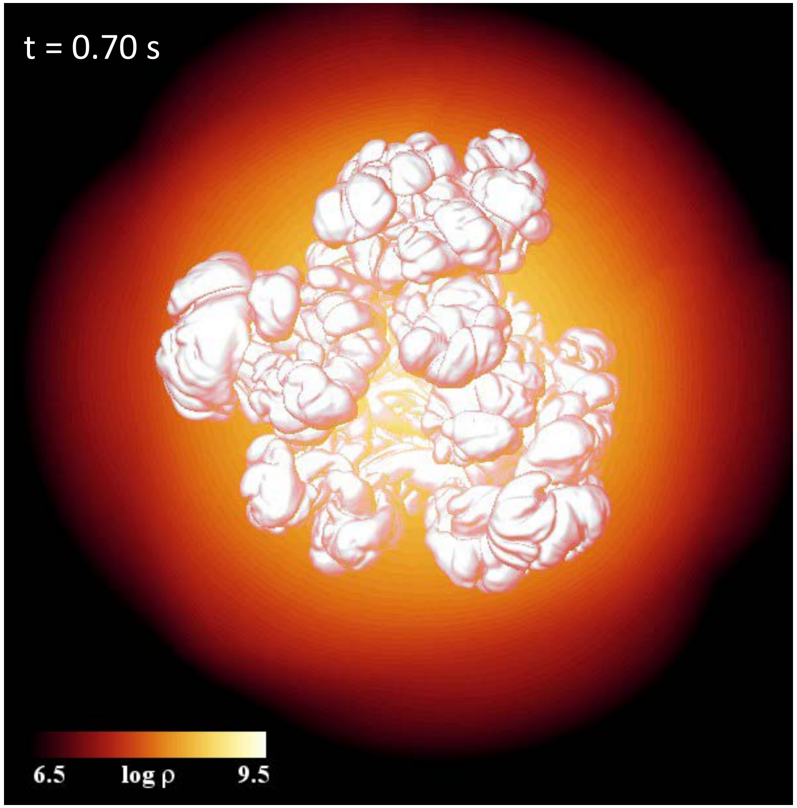

3D simulations of Type Ia supernovae

Modeling pipeline:

Progenitor scenario → Hydrodynamical simulation → Nucleosynthesis calculation → Radiative transfer calculations → Observables (lightcurves, spectra)

First simulation
(single degenerate scenario)

Delayed detonation model:
(Seitenzahl et al. 2012)

- Total ejecta mass: $1.4\,M_{\odot}$
- Produced amount of ^{56}Ni: $0.6\,M_{\odot}$

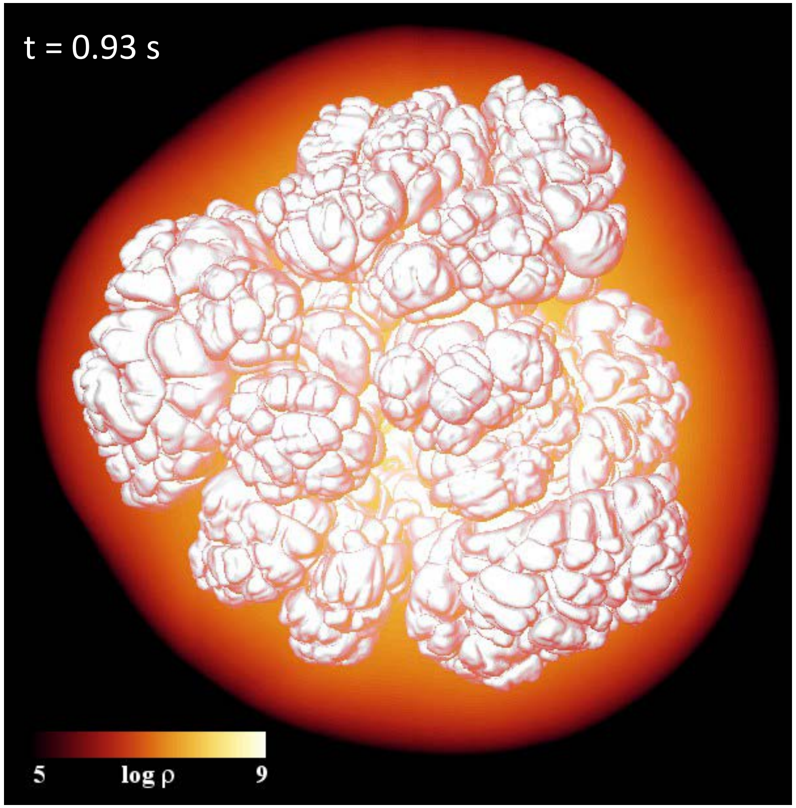

3D simulations of Type Ia supernovae

Modeling pipeline:

Progenitor scenario → Hydrodynamical simulation → Nucleosynthesis calculation → Radiative transfer calculations → Observables (lightcurves, spectra)

First simulation
(single degenerate scenario)

Delayed detonation model:
(Seitenzahl et al. 2012)

- Total ejecta mass: $1.4\,M_\odot$
- Produced amount of ^{56}Ni: $0.6\,M_\odot$

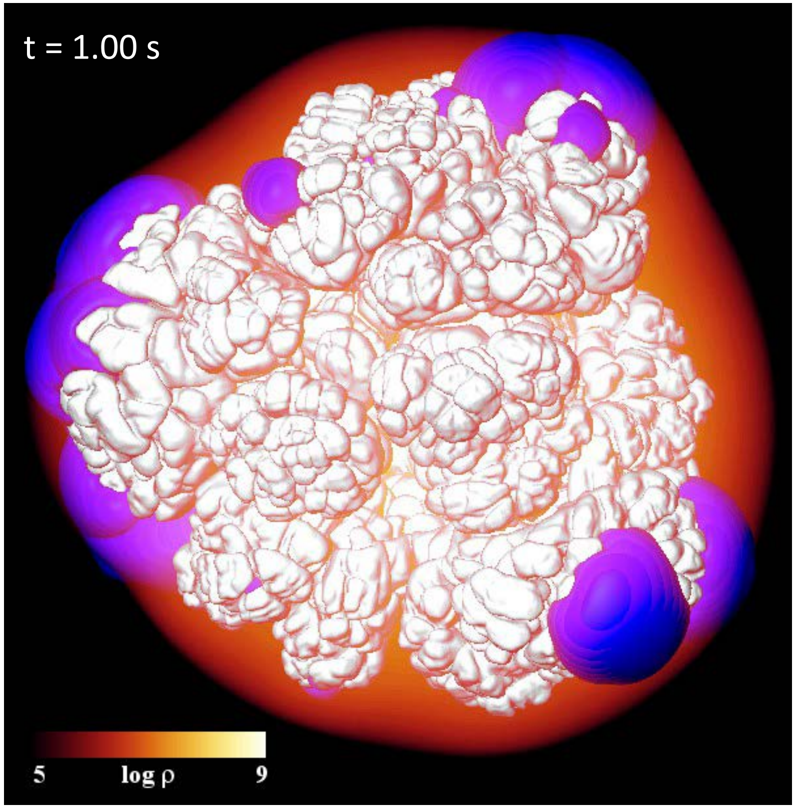

3D simulations of Type Ia supernovae

Modeling pipeline:

Progenitor scenario → Hydrodynamical simulation → Nucleosynthesis calculation → Radiative transfer calculations → Observables (lightcurves, spectra)

Second simulation
(double degenerate scenario)

Violent merger model:
(Pakmor et al. 2012)

- $M_1 = 1.1\,M_\odot,\quad M_2 = 0.9\,M_\odot$
- Produced amount of ^{56}Ni: $0.6\,M_\odot$

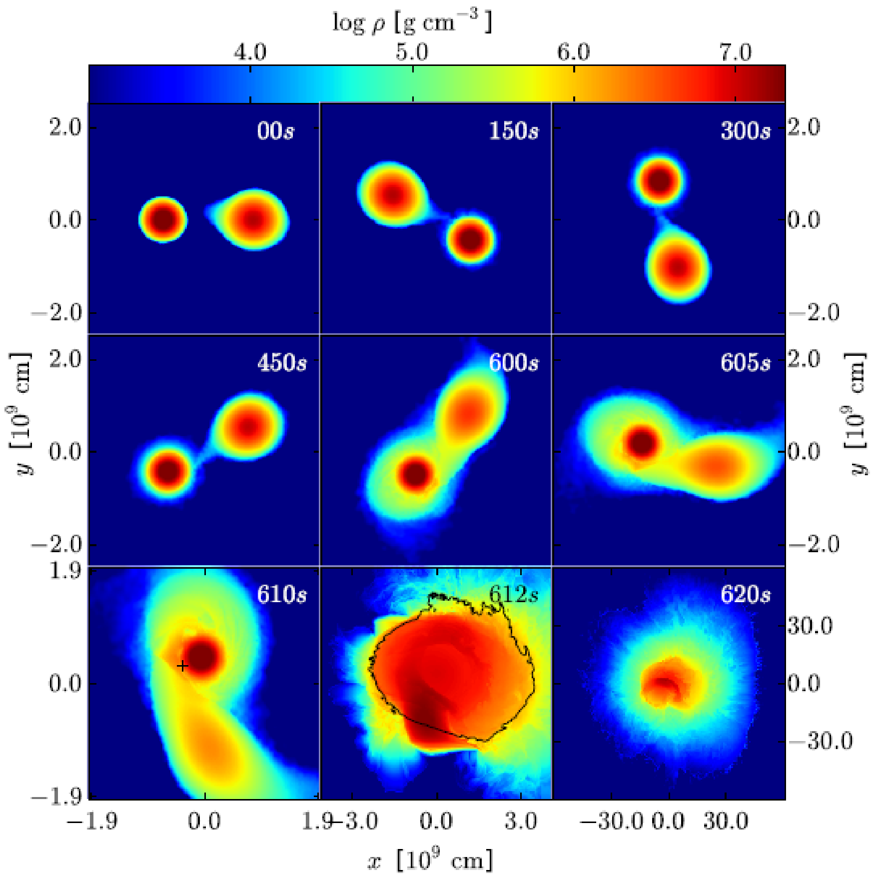

Why are Type Ia supernovae bright?

- ^{56}Ni decay chain:

$$100\,\% \quad {}^{56}\mathrm{Ni} + e^- \rightarrow {}^{56}\mathrm{Co} + \nu_e + \gamma \qquad t_{1/2} = 6.08\,\mathrm{d}$$
$$80\,\% \quad {}^{56}\mathrm{Co} + e^- \rightarrow {}^{56}\mathrm{Fe} + \nu_e + \gamma$$
$$20\,\% \quad {}^{56}\mathrm{Co} \rightarrow {}^{56}\mathrm{Fe} + e^+ + \nu_e + \gamma \qquad t_{1/2} = 77.24\,\mathrm{d}$$

- γ and e^+ from ^{56}Ni decay chain heat ejecta **(Truran 1967, Colgate & McKee 1969)**
  $\longrightarrow$ Optical emission **(e.g. Kuchner et al. 1994)**

Delayed detonation model — Violent merger model

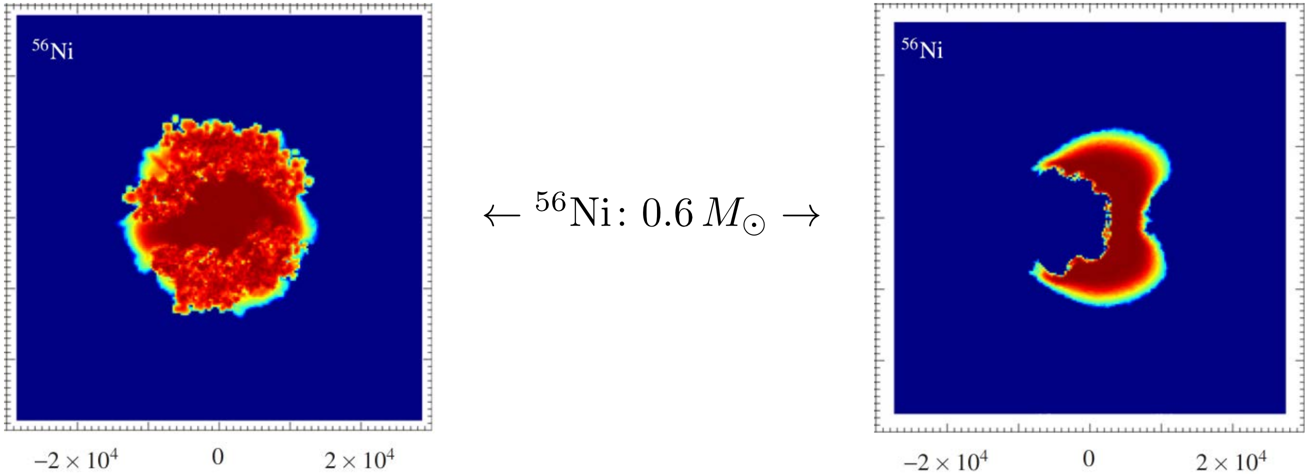

Slices through the two models in the *x*–*z*-plane showing the abundance distribution of ^{56}Ni at 100 s after explosion **(Röpke et al. 2012)**.

UVOIR lightcurves

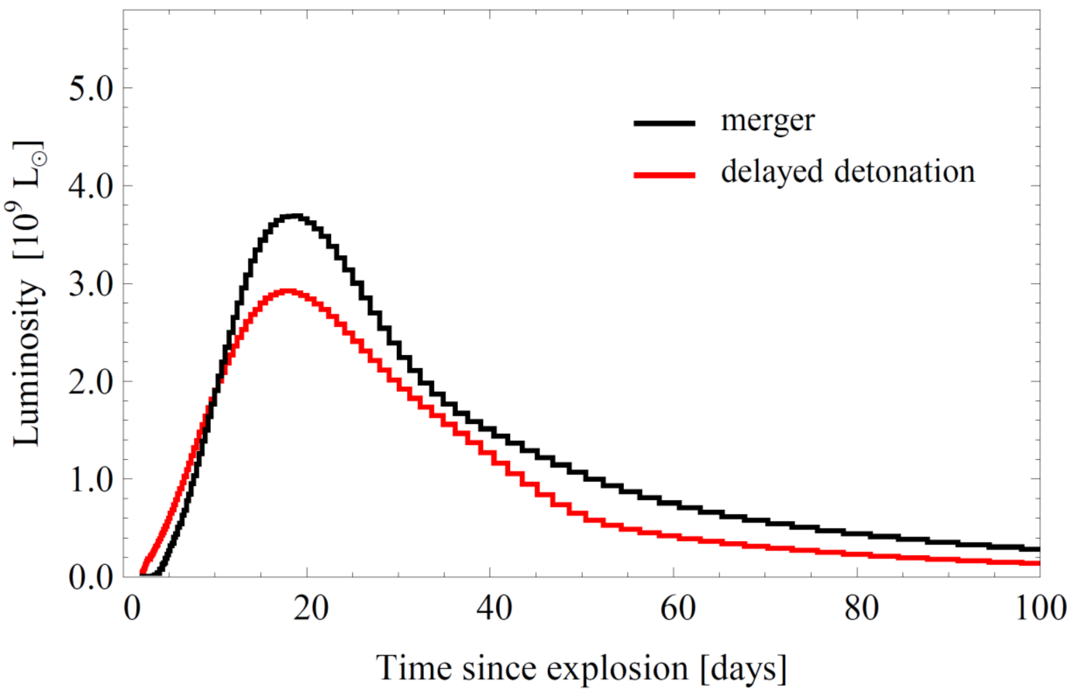

Comparison of bolometric UVOIR lightcurves from the delayed detonation and the violent merger model **(Summa et al., 2013)**.

UVOIR lightcurves

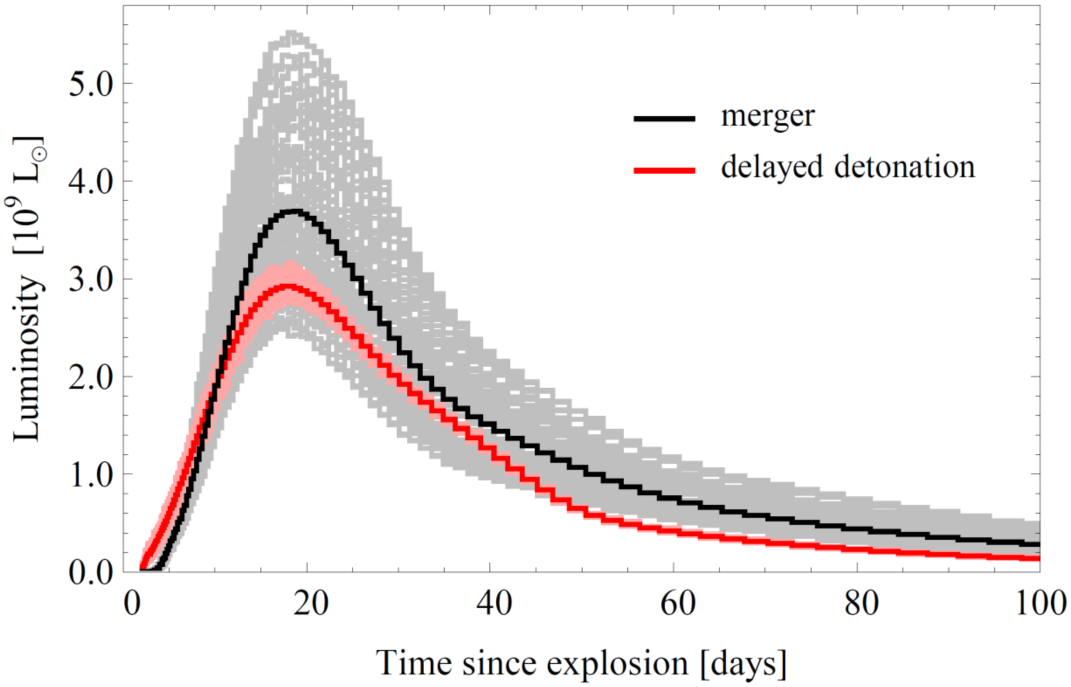

Comparison of bolometric UVOIR lightcurves from the delayed detonation and the violent merger model. The light curve spread due to different viewing angles is indicated in light red and gray **(Summa et al., 2013)**.

Gamma-ray vs. UVOIR light curves

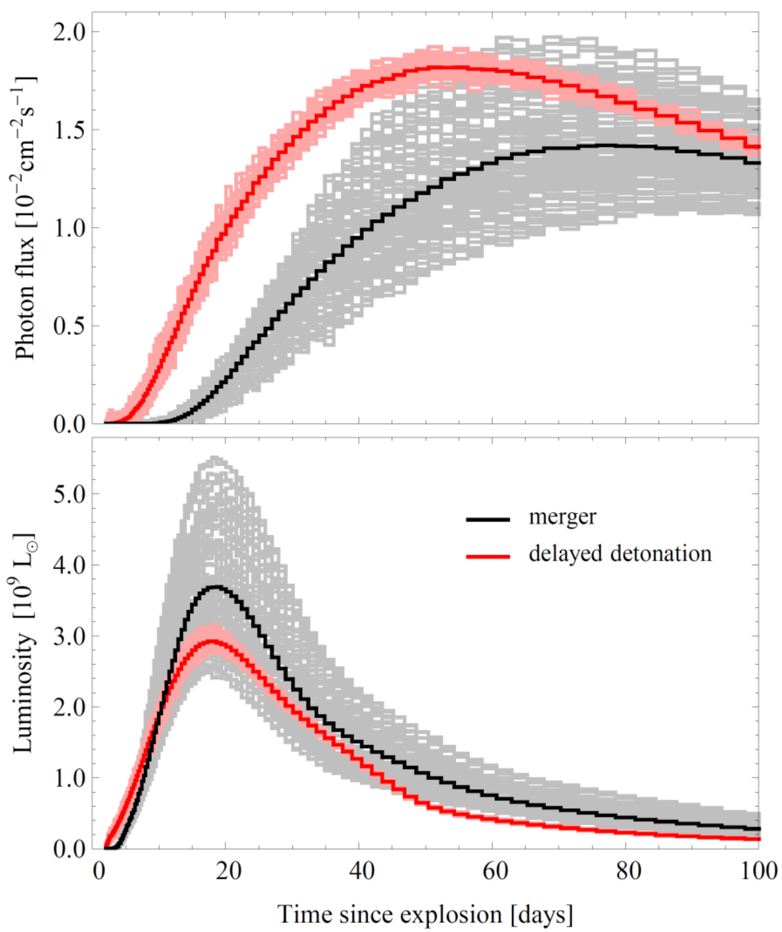

Bolometric gamma-ray light curve (upper panel) and bolometric UVOIR light curve (lower panel) for the delayed detonation (red) and the violent merger model (black). The light curve spread due to different viewing angles is indicated in light red and gray **(Summa et al., 2013)**.

Gamma-ray spectra

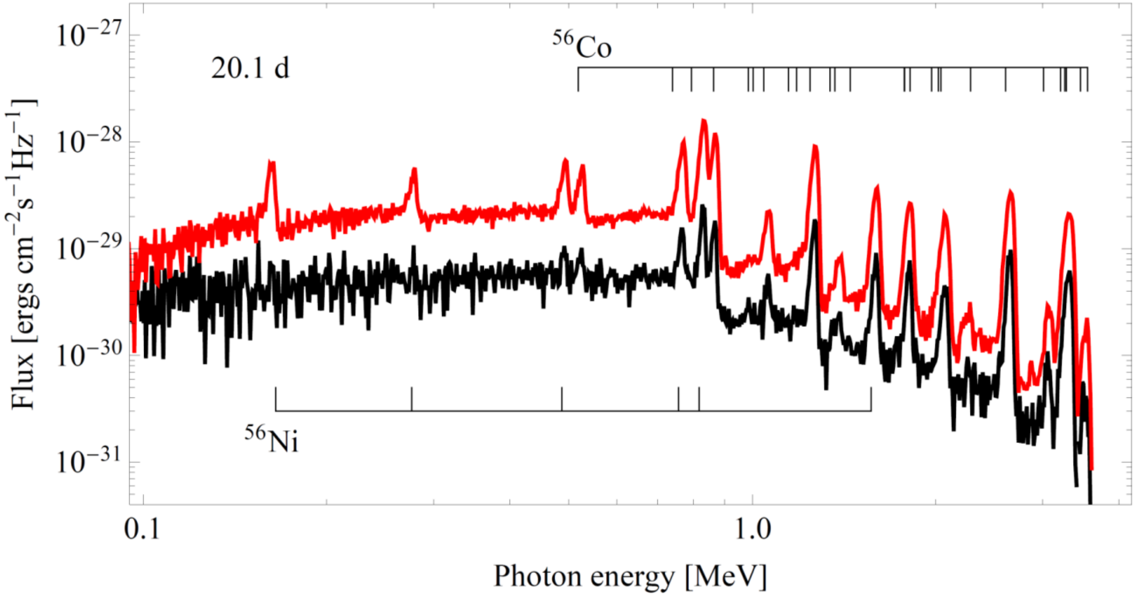

Comparison of gamma-ray spectra from the delayed detonation (red) and the violent merger model (black) **(Summa et al., 2013)**.

- Gamma-ray spectra of SNe Ia are dominated by the lines of the decay chain ^{56}Ni $\longrightarrow$ ^{56}Co $\longrightarrow$ ^{56}Fe
- Delayed detonation model: Two prominent ^{56}Ni lines (0.158 and 0.270 MeV)

$\longrightarrow$ can only build up if a significant amount of ^{56}Ni is located at small optical depths

$\longrightarrow$ Direct connection of low-energy ^{56}Ni lines to the source distribution of radioactive material

Diagnostic tools: Hardness ratios

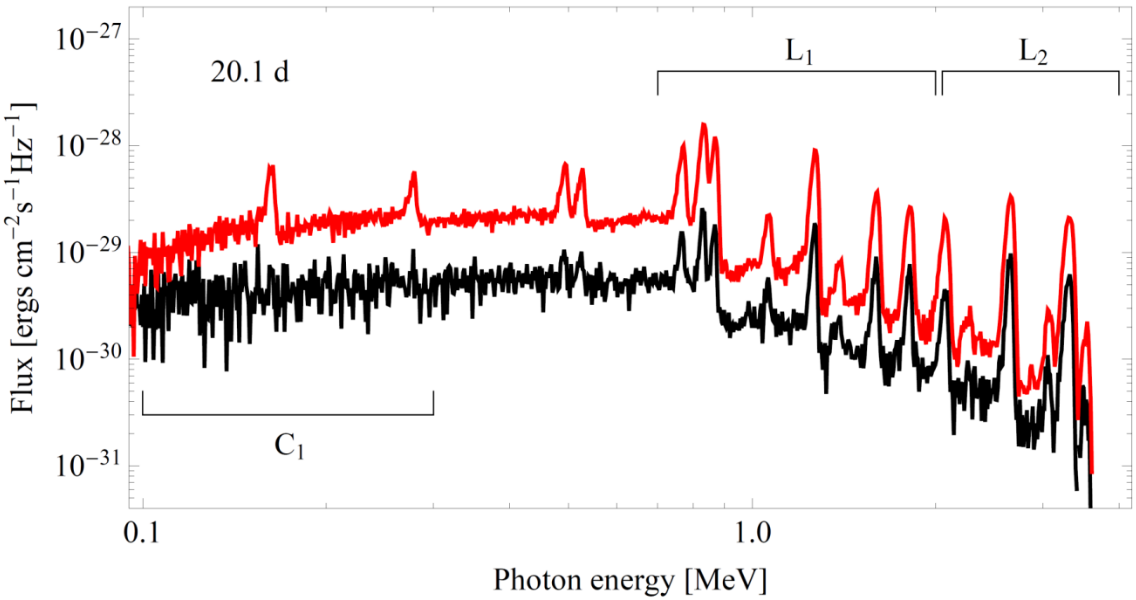

Comparison of gamma-ray spectra from delayed detonation (red) and merger model (black) **(Summa et al., 2013)**.

- Comparison of fluxes in broader energy bands
- Coarser method, but the relative simplicity of gamma-ray spectra makes them to an important diagnostic tool
- Hardness ratios are mainly effected by the energy dependence of the Compton cross section

Diagnostic tools: Hardness ratios

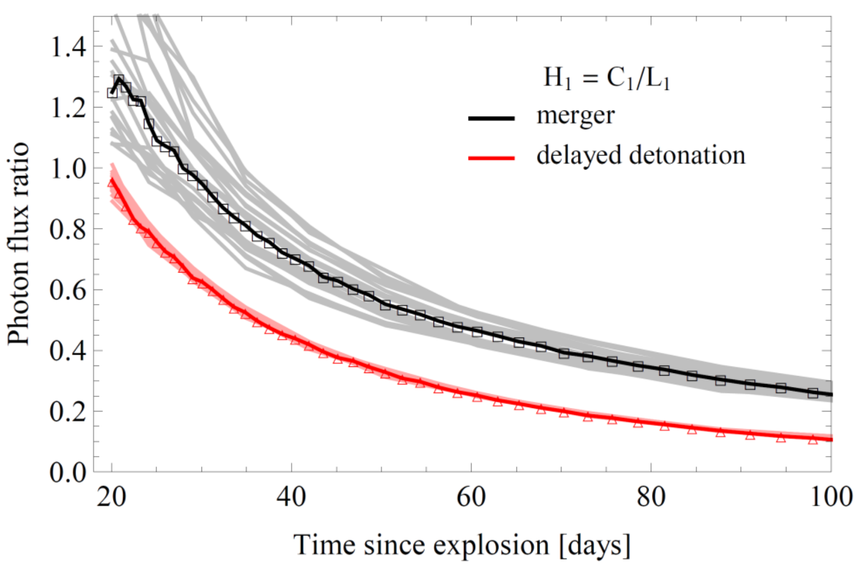

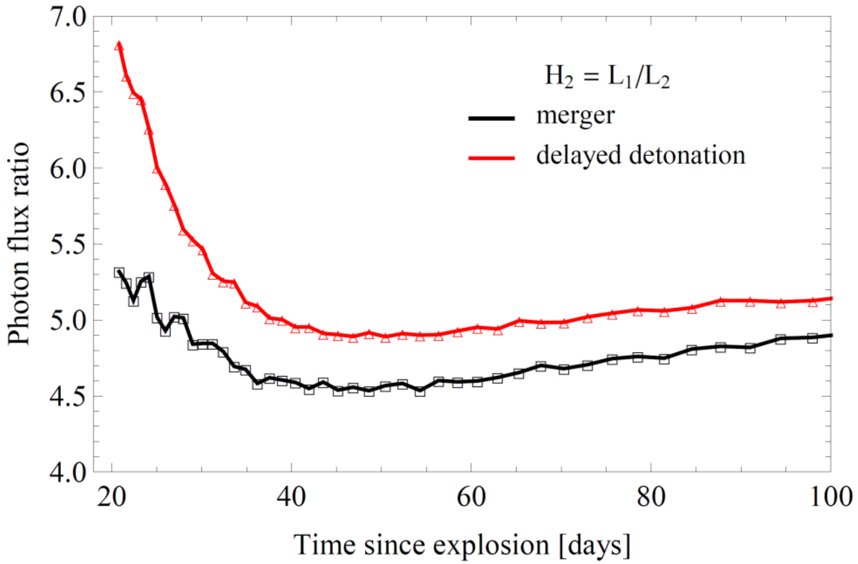

Hardness ratios of the gamma-ray emission from the delayed detonation (red) and the violent merger model (black). The light curve spread due to different viewing angles is indicated in light red and gray in the left panel **(Summa et al., 2013)**.

GRIPS detector simulations

Hardness ratios (exposure time: 10^5 s):

1 Mpc

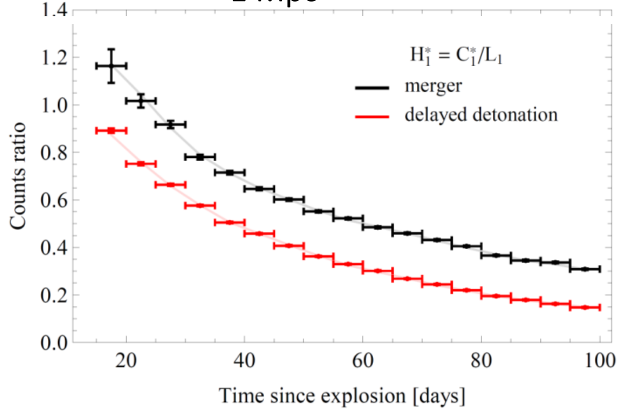

5 Mpc

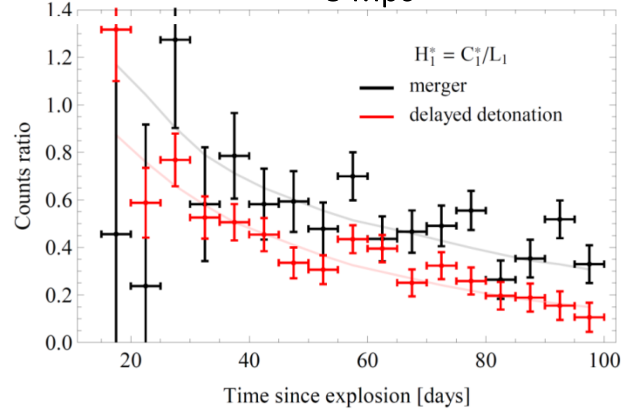

Light curves (exposure time: 10^5 s):

1 Mpc

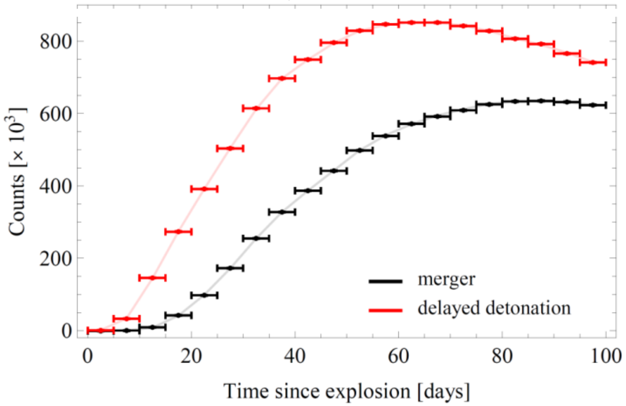

10 Mpc

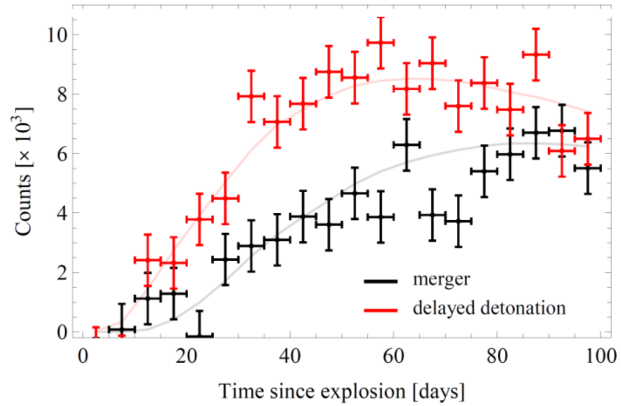

Higher exposure time of 10^6 s: Model distinction possible up to 10 Mpc (hardness ratios) or 16 Mpc (light curve measurements, **Summa et al., 2013**).

Outline

High energy observables of nuclear processes

⇕

Diagnostic tools for conclusions on astrophysical models

Two examples:

1. Nuclear lines as a fingerprint of hadronic cosmic rays
2. High-energy observables of Type Ia supernovae
   - Gamma-ray emission
   - X-ray line emission:
     5.9 keV Mn K-shell X-ray luminosity from
     the decay of ^{55}Fe in SNe Ia

Nucleosynthesis conditions in SNe Ia

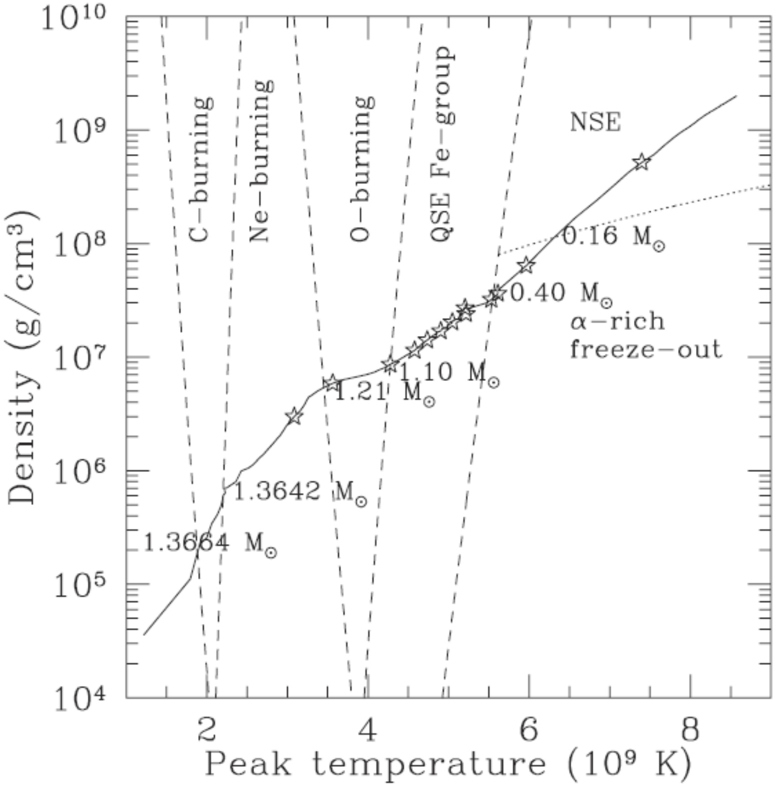

Bravo & Martinez-Pinedo 2012

Normal freeze-out from NSE:

- Low entropy, high density ($> 3 \times 10^8\,\mathrm{g\,cm^{-3}}$)
- Low fraction of light particles
- ^{55}Co survives

Alpha-rich freeze-out from NSE:

- High entropy, low density ($< 3 \times 10^8\,\mathrm{g\,cm^{-3}}$)
- High fraction of light particles
- ^{55}Co is destroyed by ^{55}Co(p,γ)^{56}Ni

Nucleosynthesis conditions in SNe Ia

- ^{55}Co: decays with a half-life of 17.5 h to ^{55}Fe
- ^{55}Fe: decays ($\tau_{1/2}$ = 2.7 yr) via electron capture to ^{55}Mn
- ^{55}Mn relaxes to eliminate K-shell vacancies

→ Emission of X-rays at 5.888 keV (8.2%) and 5.899 keV (16.2%)

Nucleosynthesis conditions in SNe Ia

- ^{55}Co: decays with a half-life of 17.5 h to ^{55}Fe
- ^{55}Fe: decays ($\tau_{1/2}$ = 2.7 yr) via electron capture to ^{55}Mn
- ^{55}Mn relaxes to eliminate K-shell vacancies

→ Emission of X-rays at 5.888 keV (8.2%) and 5.899 keV (16.2%)

Delayed detonation model

- Densities are sufficiently high for "normal" freeze-out from NSE
- ^{55}Co is abundantly synthesized

Violent merger model

- Lower peak densities
- ^{55}Co is predominantly synthesized in incomplete Si-burning

→ mass of ^{55}Co and ^{55}Fe at t = 100 s:

Delayed detonation model: $1.33 \times 10^{-2} M_{\odot}$

Violent merger model: $3.73 \times 10^{-3} M_{\odot}$

→ robust physical prediction of different ^{55}Co yields for the different explosion scenarios

Radiative transfer calculations

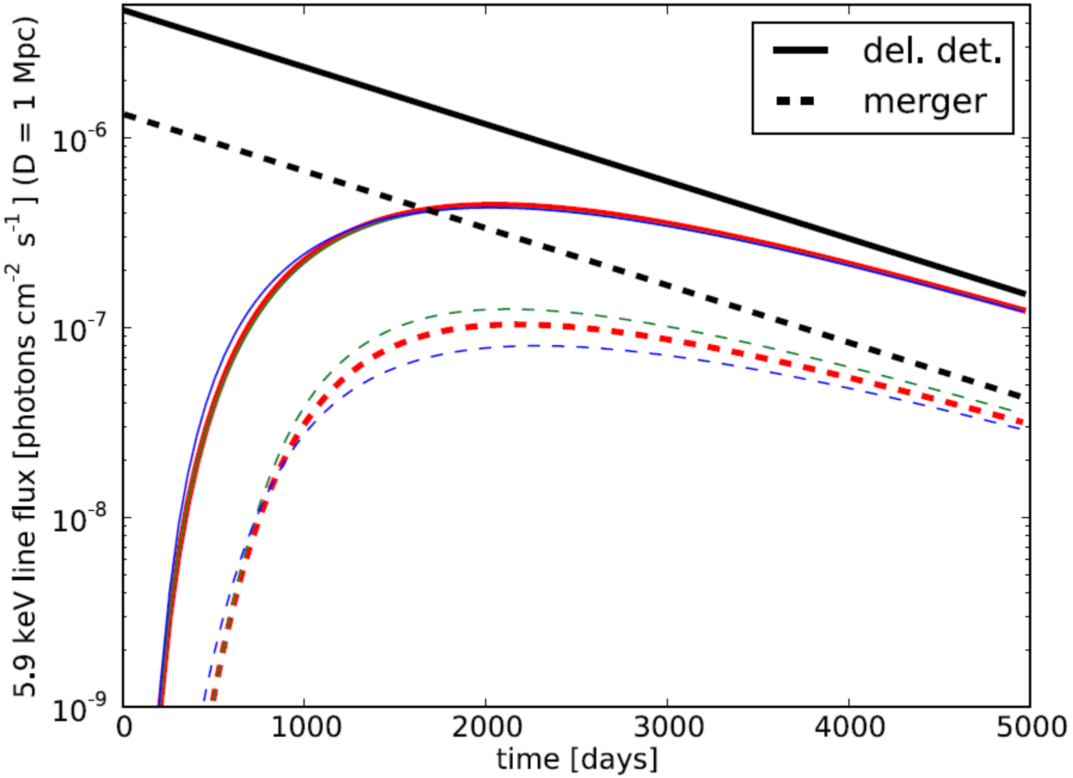

X-ray line flux for the two different explosion models at a distance of 1 Mpc. The three different colors indicate three orthogonal lines of sight. Black lines indicate the free streaming limit (no absorption).

Observability of the 5.9 keV line

Results of detector simulations:

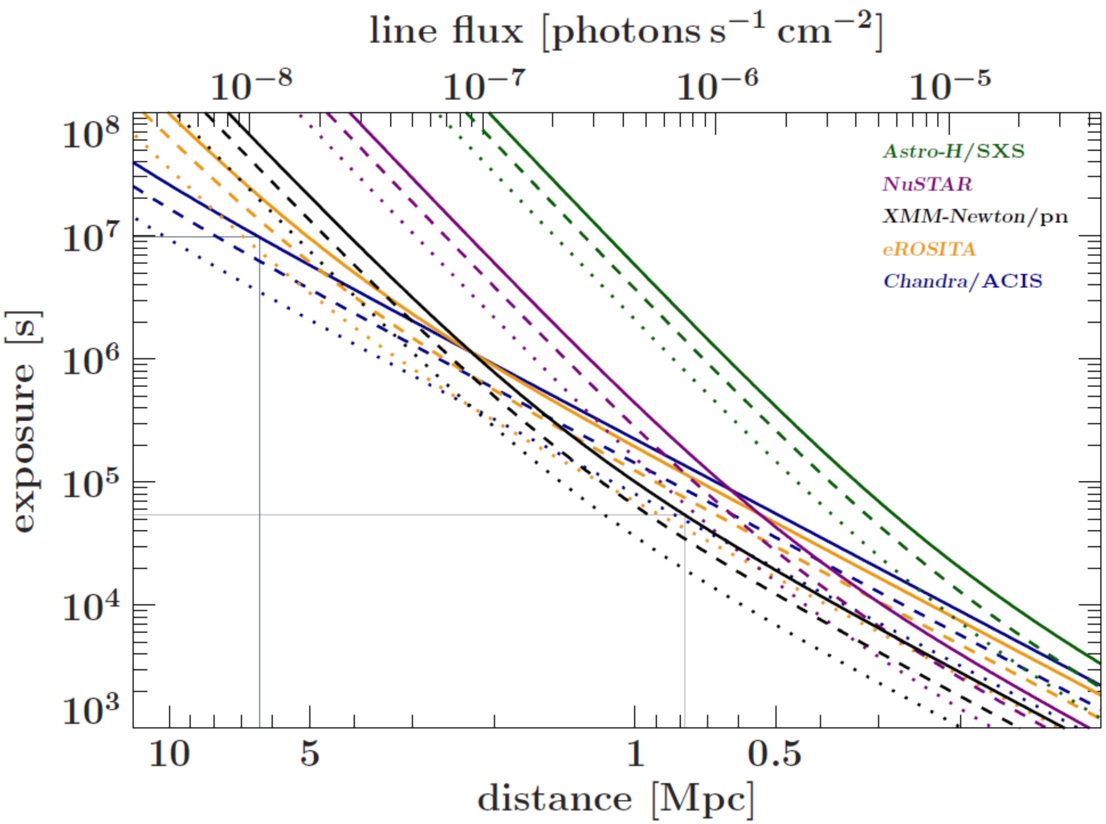

Required exposure times for the detection of the 5.9 keV line with different X-ray instruments in case of the delayed detonation model.

- For SNe Ia in the local group, a model distinction is possible for exposure times of less than 500 ks
- For exposure times of 10^6 s, a detection of the 5.9 keV line is feasible for distances up to 2 Mpc in case of the delayed-detonation model
- Proposed next-generation X-ray missions like Athena+ will further reduce these limits

Observability of the 5.9 keV line

Results of detector simulations:

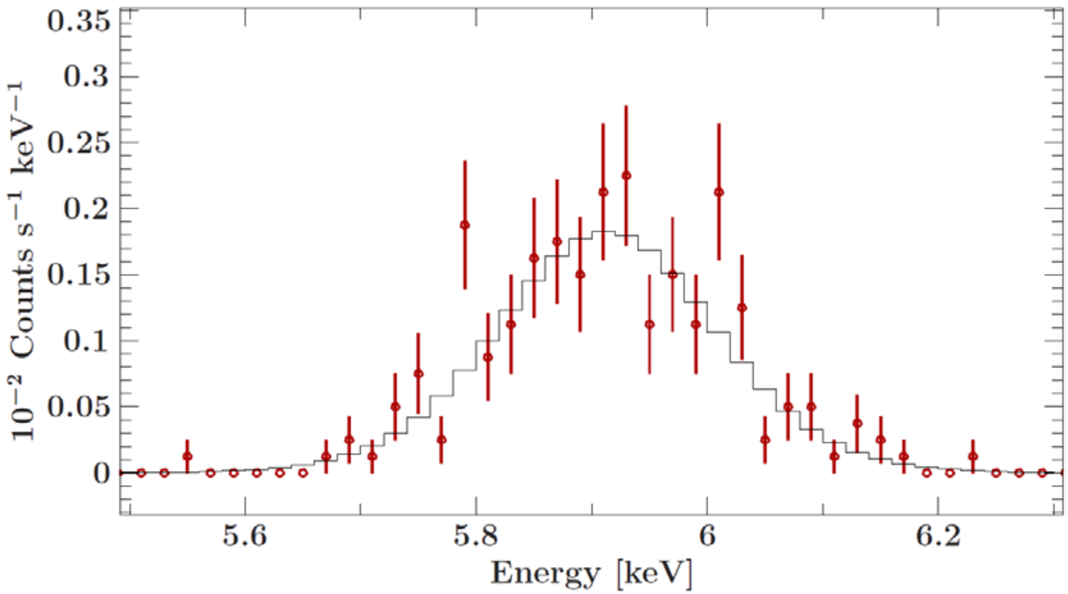

Simulated 500 ks XMM-Newton/pn background-subtracted spectrum of the 5.9 keV emission line at a distance of 0.78 Mpc.

- For SNe Ia in the local group, a model distinction is possible for exposure times of less than 500 ks
- For exposure times of 10^6 s, a detection of the 5.9 keV line is feasible for distances up to 2 Mpc in case of the delayed-detonation model
- Proposed next-generation X-ray missions like Athena+ will further enlarge these distance limits

Summary

- Distinct astrophysical models often exhibit large degeneracies in their observables

→ Clear and robust signatures that unambiguously point towards differences are necessary

- High-energy observables of nuclear processes are suited well to fulfil this purpose:
  - Nuclear de-exitation lines ↔ Cosmic ray acceleration sites
  - Early gamma-ray and X-ray line emission from radioactive nuclides in the ejecta of SNe Ia ↔ Explosion and progenitor scenarios

→ Independent diagnostic tools that can be used in addition to measurements in other wavelength regimes to constrain astrophysical models

Supernova models: SN 2011fe as a test case

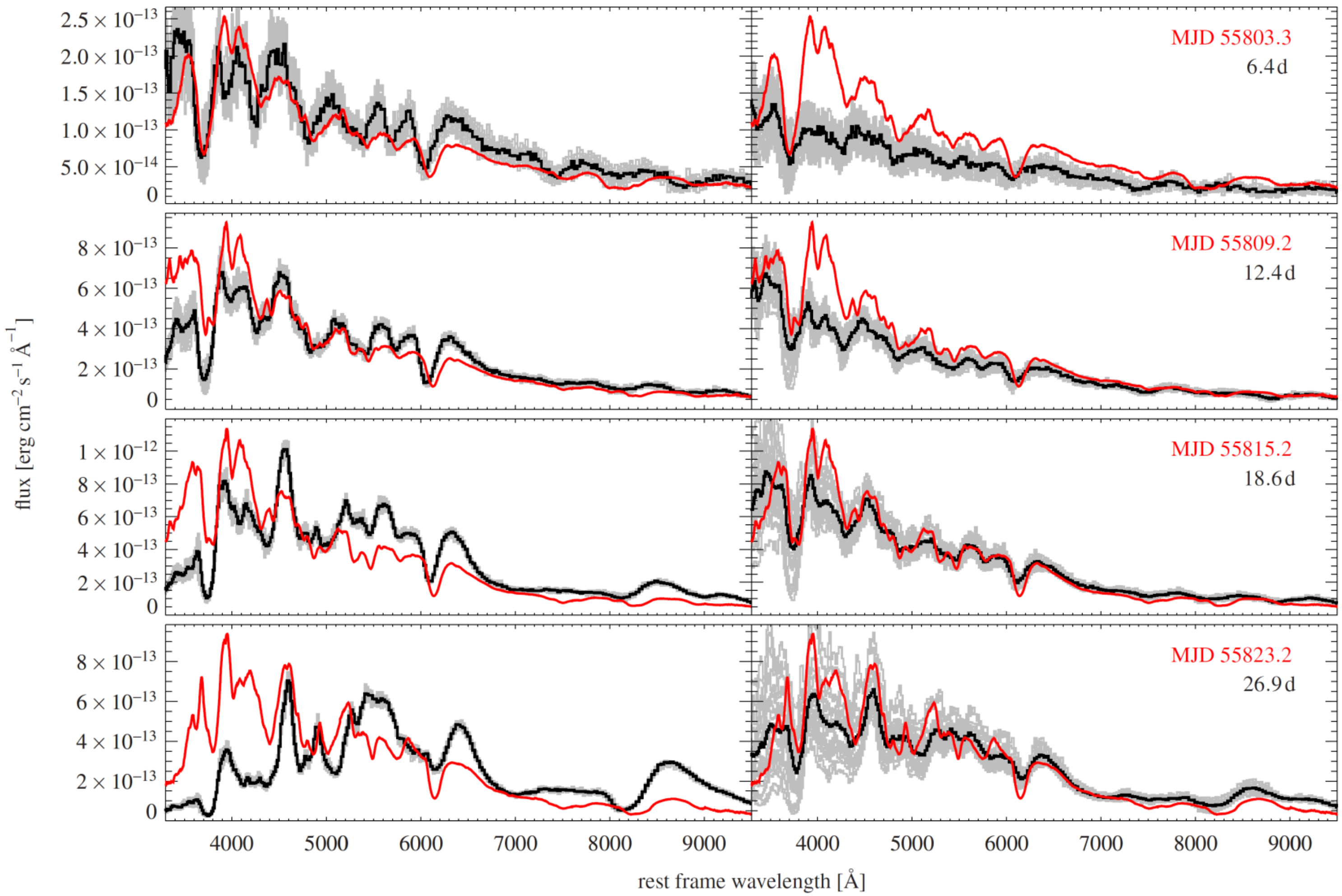

Spectral evolution of the delayed detonation (left) and the violent merger model (right) from 6 to 27 days after the explosion **(Röpke et al. 2012)**.

Detection principle

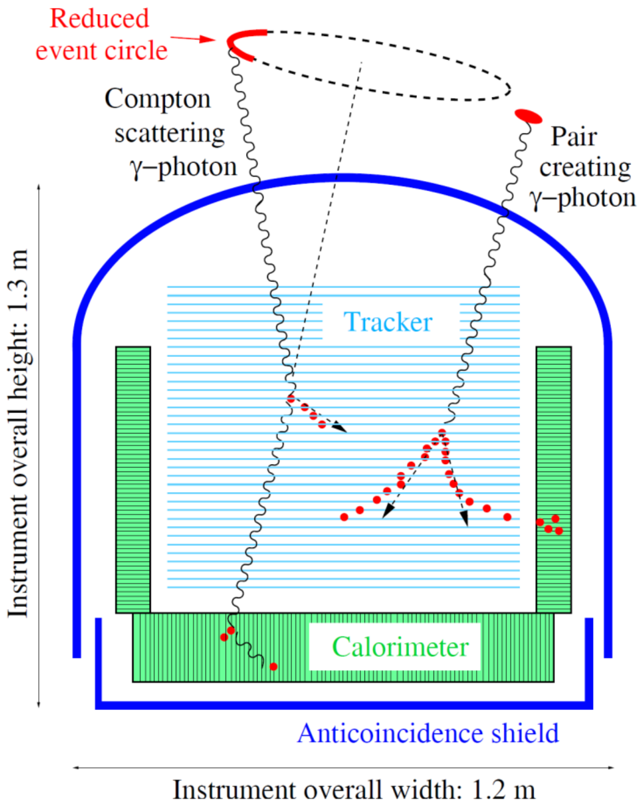

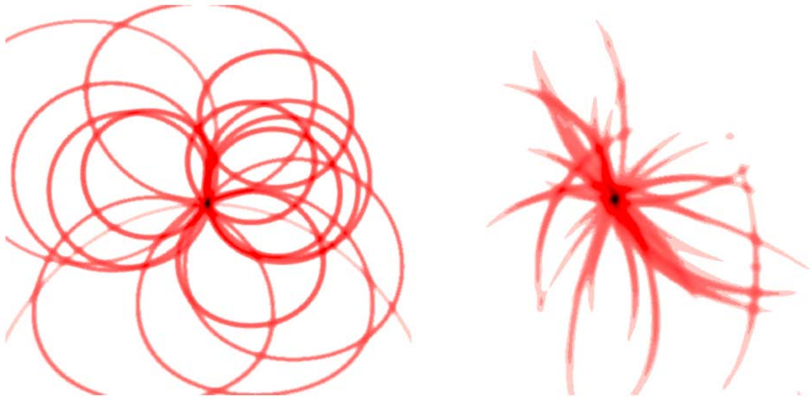

(a) Untracked Compton events

(b) Tracked Compton events

Schematic view of the working principle of GRIPS **(Andritschke, 2006)**.

Event reconstruction and imaging procedure of GRIPS **(Zoglauer, 2005)**.